



## High performing SOFC via multilayer tape casting?

Hauch, Anne

*Publication date:*  
2015

*Document Version*  
Peer reviewed version

[Link back to DTU Orbit](#)

*Citation (APA):*  
Hauch, A. (2015). *High performing SOFC via multilayer tape casting?*. Poster session presented at 10th European Fuel Cell Forum, Luzern, Switzerland.

---

### General rights

Copyright and moral rights for the publications made accessible in the public portal are retained by the authors and/or other copyright owners and it is a condition of accessing publications that users recognise and abide by the legal requirements associated with these rights.

- Users may download and print one copy of any publication from the public portal for the purpose of private study or research.
- You may not further distribute the material or use it for any profit-making activity or commercial gain
- You may freely distribute the URL identifying the publication in the public portal

If you believe that this document breaches copyright please contact us providing details, and we will remove access to the work immediately and investigate your claim.



# High performing SOFC via multilayer tape casting?

**Aim – Decreased SOFC manufacturing cost while keeping high fuel cell performance:**

Substitute processing steps that have low material yield (e.g. spraying) and those not suitable for industrial scale production.

Decrease number of sintering steps and handling efforts.

→ Multilayer tape casting (MTC) and co-sintering of support layer, anode and electrolyte could be a solution!

**Questions:**

- Can the entire anode half cell be produced via multilayer tape casting?
- Can we co-cast anode and electrolyte layers at thicknesses of just 10-15µm?
- Can we obtain optimal microstructures for all half cell components in one single sintering step providing high performing anodes?

## Microstructure

### The MTC anode half-cell

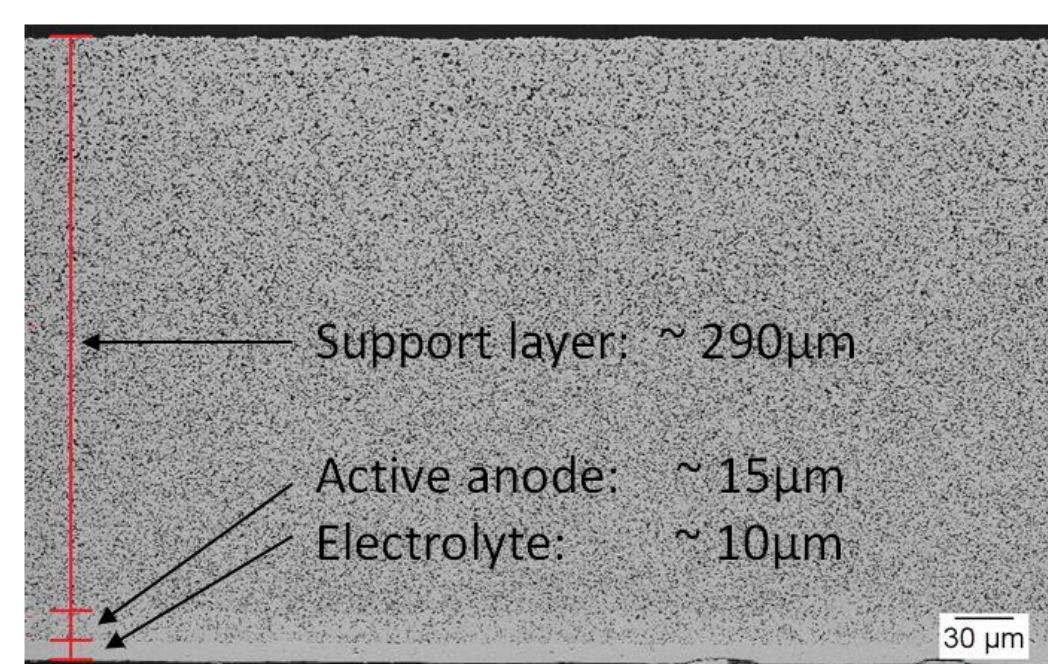


**Figure 1:** High voltage SE-detector SEM image of reduced, non-tested MTC half-cell sintered at 1315°C.

### Low voltage SEM: The percolating Ni network

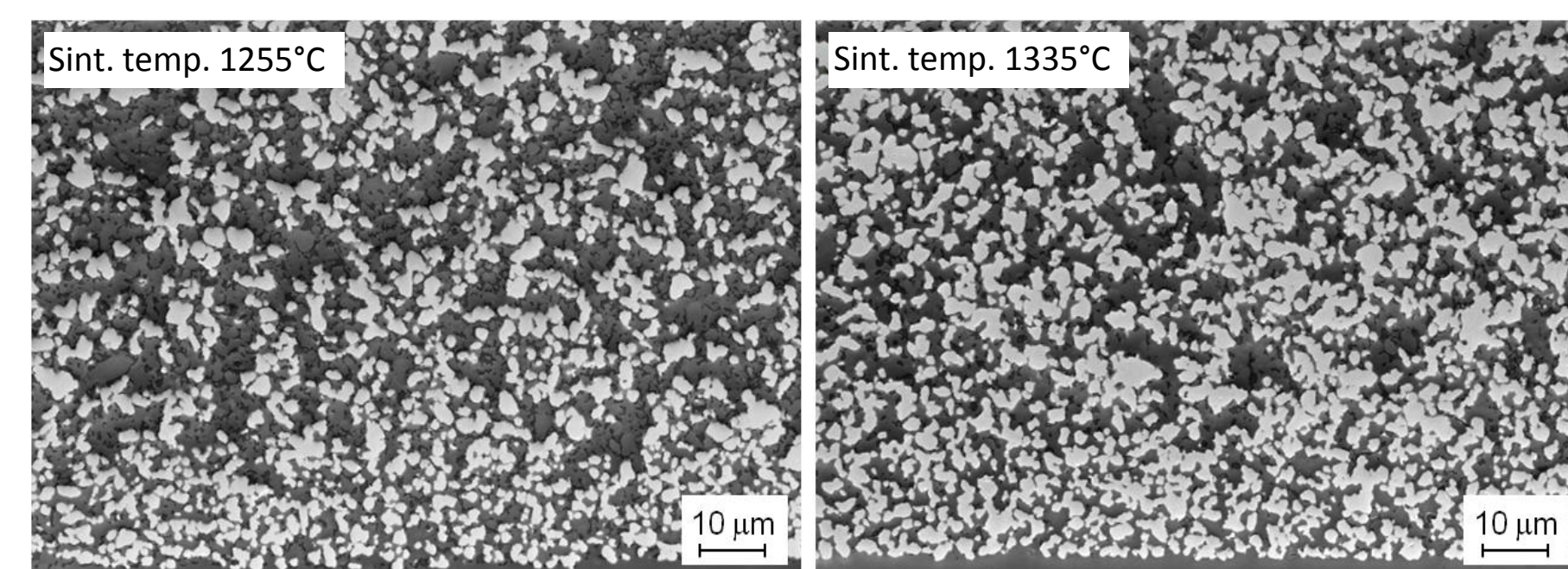


**Figure 2:** Low voltage (0.9kV) in-lens SEM images of reduced, non-tested MTC half cells. Bright particles constitute the percolating Ni-network.

### High voltage SEM: Impact of sint. temperature

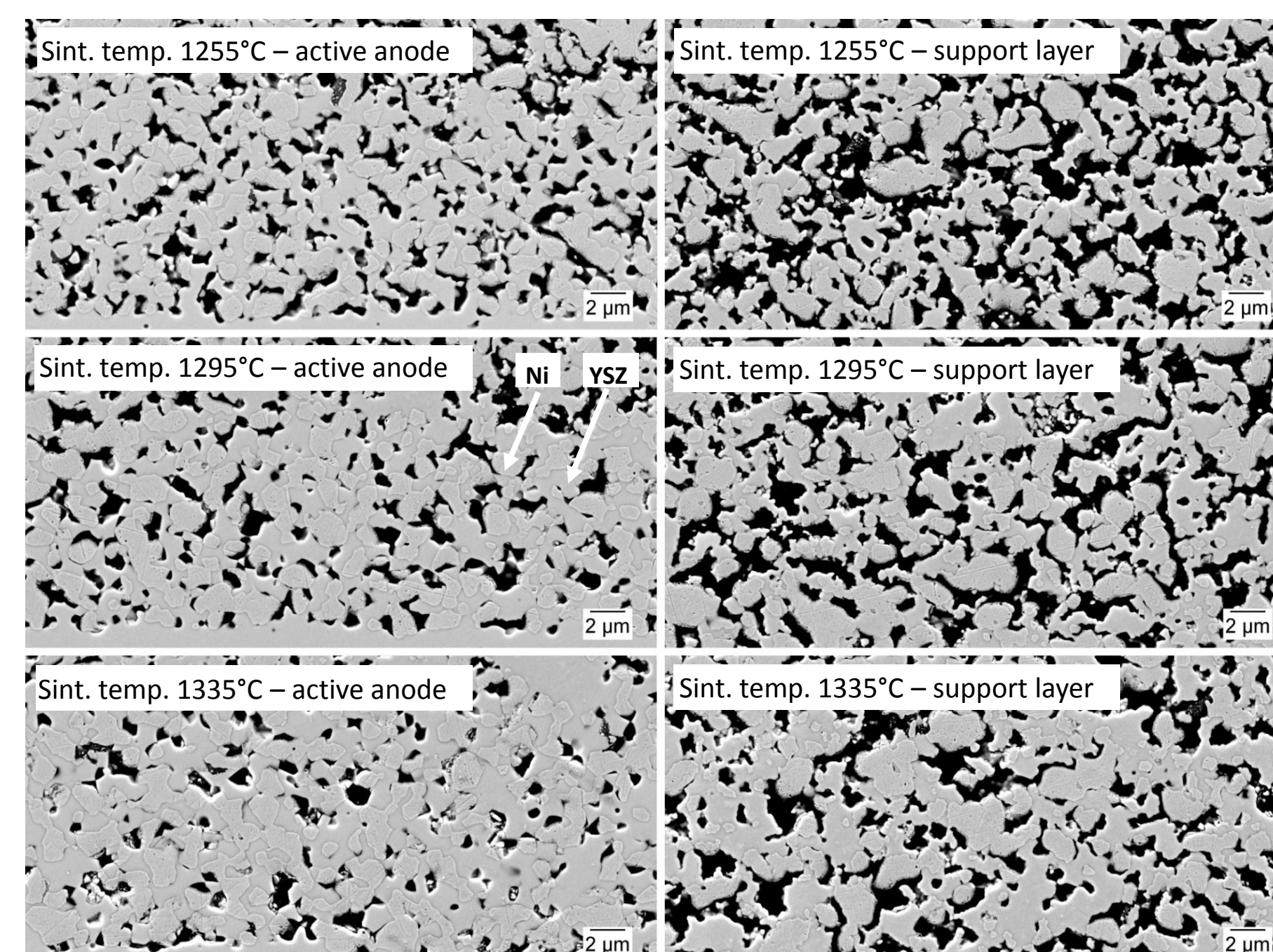


**Figure 3:** High voltage (8 kV) SE-detector SEM images of reduced, non-tested MTC half-cells. Pores appear black. Ni and YSZ phases are designated in the image of the 1295-cell.

### Microstructural analysis: Phase fractions and mean intercept lengths

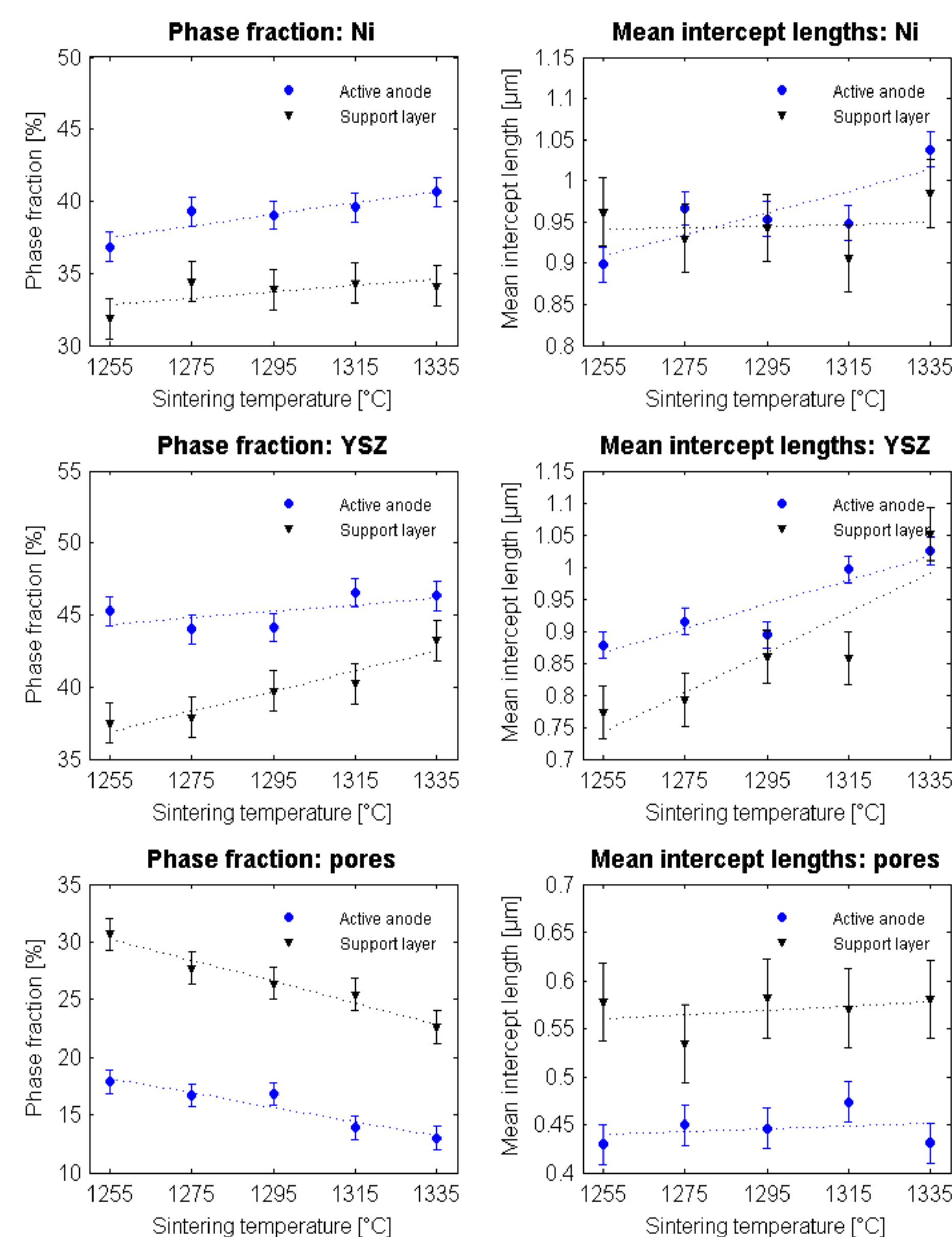


**Figure 4:** Microstructural analysis of reduced, non-tested half-cells sintered at 1255°C, 1275°C, 1295°C, 1315°C and 1335°C. Uncertainties for the measured intercept lengths are app.  $\pm 0.04\mu\text{m}$  and  $\pm 1.4\%$  for phase fractions. Measurements were performed on high voltage SE-detector images, at 11.3 kX (Figure 3), using in-house developed Matlab-based software ManSegv0.31. A minimum of 1000 line intercepts were measured for each phase in anode and support of all 5 cell samples.

## Findings

DTU Energy Conversion produce SOC anode half-cells by MTC and co-sintering in a pre-pilot plant. Investigations of microstructure and performance of cells (Ni/3YSZ-Ni/8YSZ-8YSZ-LSM/YSZ) with MTC anodes reveal:

- 1) A “window” for the co-sintering from 1255°C to 1335°C
- 2) Uniform microstructures of desired thicknesses, porosities, particle sizes and percolation
- 3) High initial performance
- 4) Correlations of microstructure and performance with sintering temperature — increased porosity and decreased Ni particle size with lower sintering temperature  $\Rightarrow$  decreased gas diffusion and charge transfer reaction resistance in the Ni/YSZ anode half cell.

## Electrochemical performance

### Performance analysis: EIS, DRT, iV

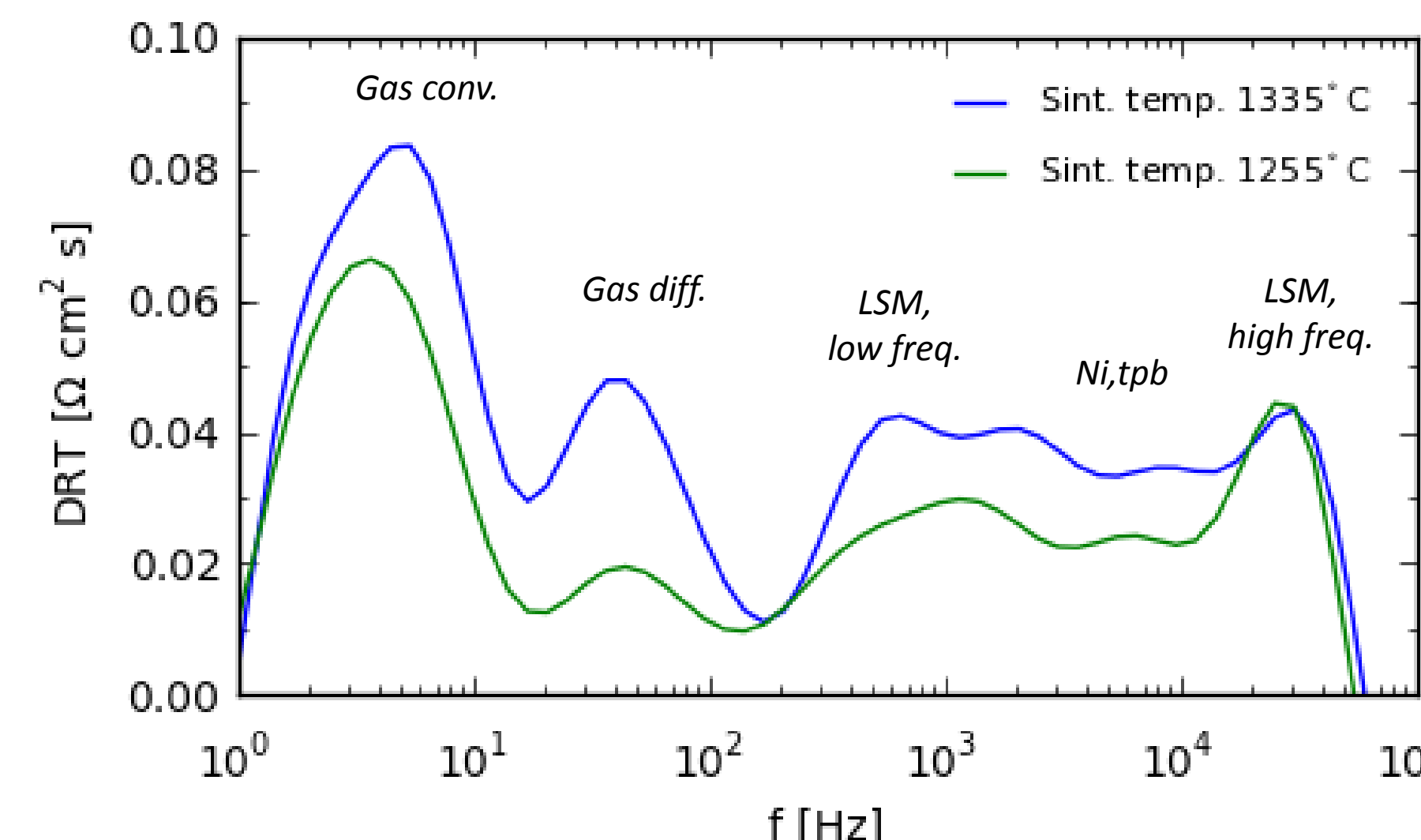
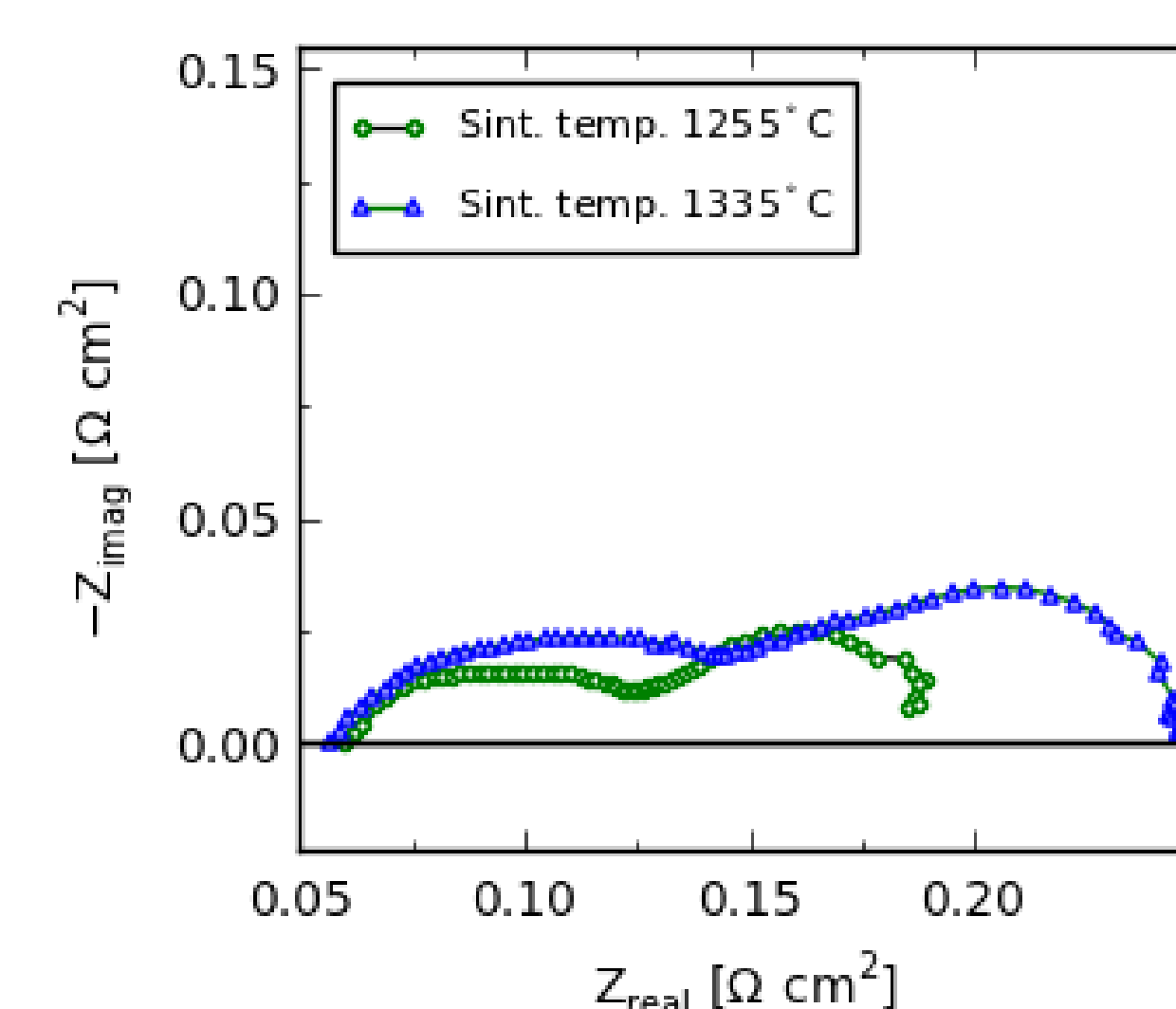


**Figure 5:** Nyquist (left) and DRT plot (right) of impedance spectra (IS) at 850°C, OCV, air to the cathode, 21-23%  $\text{H}_2\text{O}$  in  $\text{H}_2$  to the anode. The Nyquist plot is corrected for inductance.

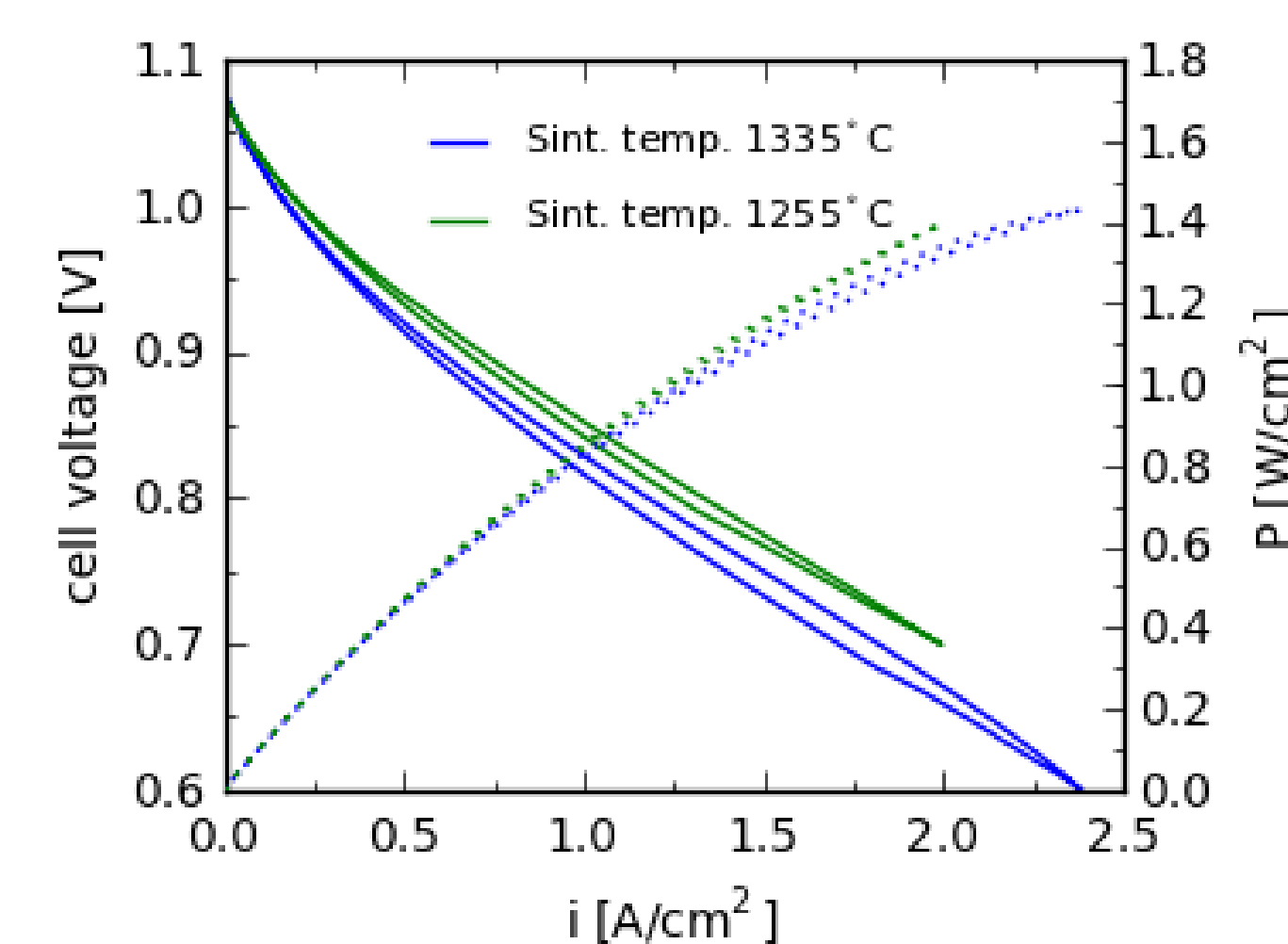


**Figure 6:** IV curves at 850°C, air to the cathode, 4%  $\text{H}_2\text{O}$  in  $\text{H}_2$  to the anode.

### EIS analysis: CNLS fitting

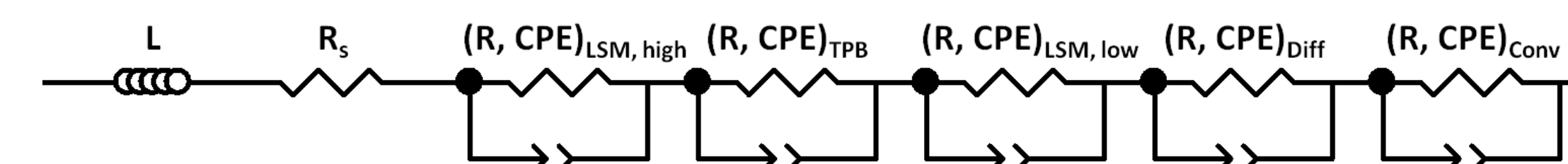


**Figure 7:** Equivalent circuit model applied in CNLS fitting of IS shown in Figure 5. Inductance L and series resistance  $R_s$  are connected in series with 5 RQ elements, representative of the polarisation resistance. Corresponding results are given in Table 1.

Sint. temp.	ASR <sub>FU</sub> (mΩcm <sup>2</sup> )	R <sub>s</sub> (mΩcm <sup>2</sup> )	R <sub>tpb</sub> (mΩcm <sup>2</sup> )	f <sub>s,tpb</sub> (Hz)	R <sub>Diff</sub> (mΩcm <sup>2</sup> )	f <sub>s,Diff</sub> (Hz)	R <sub>Conv</sub> (mΩcm <sup>2</sup> )	f <sub>s,Conv</sub> (Hz)
1255°C	128	51	52	8442	15	39	51	4
1335°C	158	42	85	7112	34	39	61	4

**Table 1:** ASR<sub>FU</sub> at 700 mV from iV-curves in Figure 6 and resistances and summit frequencies from CNLS-fit of the IS shown in Figure 5. Estimated error for the resistances  $\sim 3 \text{ m}\Omega\text{cm}^2$ .

## Sintering temperature: 1255°C → 1335°C

### Microstructure



### Cell performance

- 1) Lower porosity  
(support: from 31% to 23%; active anode: from 18% to 13%)
- 2) Ni particle coarsening  
(active anode: from 0.88  $\mu\text{m}$  to 1.03  $\mu\text{m}$ )

- 1)  $\sim 2$ -fold increase in gas diffusion resistance
- 2) Increase in charge transfer reaction resistance from 52 mΩcm<sup>2</sup> to 85 mΩcm<sup>2</sup> (850 °C)